Fibers and Polymers 2017, Vol.18, No.4, 611-618
DOI 10.1007/s12221-017-6921-5

ISSN 1229-9197 (print version)
ISSN 1875-0052 (electronic version)

Thermal, Swelling and Stability Kinetics of Chitosan Based Semi-Interpenetrating Network Hydrogels

Muhammad Omer Aijaz[1], Sajjad Haider[2]*, Fahad S. Al-Mubaddel[2], Rawaiz Khan[2], Adnan Haider[3], Abdulaziz Abdullah Alghyamah[2], Waheed A. Almasry[2], Mohammad Sherjeel Javed Khan[4], Muhammad Javid[5], and Wajahat Ur Rehman[6]

[1]*Center of Excellence for Research in Engineering Materials, Advance Manufacturing Institute, King Saud University, Riyadh 11421, Saudi Arabia*
[2]*Department of Chemical Engineering, College of Engineering, King Saud University, Riyadh 11421, KSA, Saudi Arabia*
[3]*Department of Nano, Medical and Polymer Materials, College of Engineering, Yeungnam University, Gyeongsan 38541, Korea*
[4]*Department of Chemistry, Kyungpook National University, Daegu 41566, Korea*
[5]*Chemistry Division PAEC Islamabad, 44000, Pakistan*
[6]*Department of Chemical Engineering, UET, KPK Peshawar, 25000, Pakistan*
(Received September 16, 2016; Revised November 18, 2016; Accepted November 26, 2016)

Abstract: The present study is focused on studying the swelling kinetics, thermal and aqueous stabilities, and determination of various forms of water in the chitosan (CS) and polyacrylonitrile (PAN) blend and semi-interpenetrating polymer network (sIPN). CS/PAN blend hydrogel films were prepared by solution casting technique. The blend film with optimum swelling properties was selected for the synthesis of sIPN. CS in the blend was crosslinked with the vapors of Glutaraldehyde (GTA) to prepare sIPN. The fabricated CS/PAN blend and sIPN hydrogels films were characterized with Fourier transform infrared (FTIR), thermal gravimetric analysis (TGA) and field emission scanning electron microscope (FESEM). The kinetics of swelling, bound and unbound waters and aqueous stability were determined experimentally. FESEM showed good miscibility between CS and PAN, FTIR showed no chemical interaction between CS and PAN; however, it did show a doublet for the sIPN, TGA showed improved thermal stability and swelling kinetic followed second order kinetics. The degree of swelling of the sIPN hydrogels samples at room temperature varied from ~2200 % (with a fair degree of stability (~30 %)) to ~1000 % (with high degree of aqueous stability (43 %)) with increase in the crosslinking time. The calculated unbound water (W_{UB}) max., for the blend was 52.3 % whereas for the bound (W_B) the max., was 41.9 %. However, for sIPN hydrogel films, the W_{UB} water decreased (max. 21.0 %) where as the W_B increased (max. 52.0 %). The decrease in W_{UB} and increase in the W_B is attributed to the formation of a compact structure and increase in the contact area between the water and polymers in sIPN hydrogels due to the induction of new water contacting point in these hydrogel films, respectively.

Keywords: Chitosan, Crosslinking, sIPN hydrogel, Swelling kinetics, Bound and unbound water, Thermal stability

Introduction

Recently, researchers have shown a great interest in the synthesis of materials with the capacity to absorb massive amount of water without dissolution. These materials are defined as super absorbents (hydrogels (swelling polymers)). Hydrogels are crosslinked hydrophilic polymers networks, which can absorb and retain aqueous fluids within their structure without dissolution [1,2]. Super absorbent hydrogels are hydrophilic three dimensional networks that can absorb water upto thousand times of their dry weight [1]. Certain groups, which form the polymer backbone or lateral chains such as hydroxyl (-OH), carboxylic (-COOH), primary amidic ($-CONH_2$), secondary amide (-CONH-), sulphonic ($-SO_3H$), etc., are considered to be responsible for the hydrophilicity of the network [3]. The extent of crosslinking, elasticity of the network and polymer porosity are mainly responsible for the swelling properties of the hydrogels [4]. An important aspect of hydrogels is that upon exposure to and removal of stimuli (temperature, pH, solvent composition, ionic strength, magnetic, electric fields, etc) [5], these hydrogels have demonstrated reversible transformation which enabled them to have promising applications in bioengineering applications including artificial muscle, drug delivery and many other applications e.g., switches, chemical valves, electromechanical engines, agriculture, sealants, air-fresheners, toy, etc) [6]. The preparation of hydrogels from a variety of materials including synthetic (e.g., polyethylene glycol (PEG), polyvinyl alcohol (PVA), polyhydroxy-ethylmethacrylate (PHEMA), Poly(acrylic acid) (PAA), polymethyl acrylate (PMA), polyacrylamide (PAM), methacrylic acid (MAA) copolymers) [7] and natural materials (e.g., polysaccharides, cellulose, proteins, chitosan, etc.) has been reported in the literature [8-10]. These materials possess a great package of advantages such as biocompatibility, low toxicity and susceptibility to enzymatic degradation. Having said this, researchers are still faced with some limitations, which need to be overcome. These limitations includes low

*Corresponding author: shaider@ksu.edu.sa

mechanical strength, hard to handle, difficult to load, sterilization, immunogenicity and the potential risk of transmitting animal-originated pathogens, etc. Furthermore, most of the crosslinkers are toxic in nature and when used in solution; are difficult to remove, hence there is an urgent need to control the excess of crosslinkers.

CS is a polyamino-saccharide cationic natural functional biopolymer with a repeating structural unit of 2-acetomido-2-deoxy-β-D-glucose. It is produced by the alkaline N-deacetylation of chitin. CS offers special characteristics such as biocompatibility, hydrophilicity, bioactivity, non-antigenicity, and non-toxicity (its degradation products are natural metabolites) [11]. However, like most natural polymer, CS has also shown some limitations. These limitations include instability in an aqueous medium due to the salt formation between ammonium (-NH_3+) ions along the CS chains and the carboxylate (-COO-) ions of the acetic acid (which is the solvent of CS). The salt derivatives of CS are readily soluble in the aqueous medium and therefore cannot be used as a practical material. Crosslinked CS can form rigid gel with rather weak properties.

CS properties can be improved by blending it with synthetic and natural polymers [12-14]. CS blending with other polymers can be carried out by two methods: 1) solution blending and 2) melt blending; however, solution blending is considered to be the most effective method for the preparation of CS blends [15-17]. The choice of polymer to be blended with CS varies with respect to the properties required. For instance, PEG and PVA have been blended with CS for modifying hydrophilicity [18,19]. Similarly, polyamides, poly(acrylic acid), gelatin, silk fibroin and cellulose have been used for increased mechanical properties. Moreover, in solution blending, either CS is crosslinked by using crosslinking agents to prepare semi-interpenetrating net work (sIPN) [20] or both polymers are crosslinked to prepare interpenetrating net work (IPN) [21,22]. This was done with aim to enhanced its solution stability/degradability and mechanical properties [23]. Many blends of CS with other natural and synthetics polymers have been studied to overcome the weak properties (rigidity and instability in aqueous medium) of CS based hydrogels. However, a real solution to find out the best CS/polymeric blend ratio, which could overcome these limitations, is still at large.

This study is the part of our continuous work on CS/PAN blend and sIPN hydrogel system [24]. This article mainly focuses on the vapors based crosslinking of the CS in the CS/PAN blend and the evaluation of the swelling behavior (degree of swelling, swelling kinetic and the states of water), morphology, degree of stability and thermal behavior of the blend and sIPN hydrogel films. The vapors based crosslinking of CS was previously used for nanofibers mats [25,26]. We believe that the blend and sIPN hydrogels films will be a step forward in the use of these materials in various potential applications, particularly in dye adsorption.

Experimental

Materials

Medium molecular weight (M_w) CS powder ($C_8H_{13}NO_5$)n, average M_W 150,000 PAN (C_3H_3N)n, acetic acid ($C_2H_4O_2$) ACOH), dimethyl sulfoxide ((C_2H_6OS), DMSO), absolute ethanol ((C_2H_5OH) ETOH), and sodium hydroxide (NaOH) were purchased from Sigma-Aldrich, Alfa Aesar, Paneac Quimica SAU and Scharlab S.L., respectively. GTA ($C_5H_8O_2$) was purchased from Loba Chemie. All the chemicals were of analytical grade and were used without further purification. Distilled water was used for the preparation of solutions.

Preparation of CS/PAN Hydrogel Film

CS solutions at 2 wt% concentration were prepared by dissolving CS in 2 wt% ACOH *via* a magnetic stirrer (Model Cerastir 30539) at 45 °C for 2 h. After dissolution, the solutions were filtered through a mesh with 0.063 mm pore size to obtain homogeneous solution and remove any undissolved particles. PAN at 2 wt% concentration was dissolved in DMSO *via* a magnetic stirrer (Model Cerastir 30539) at room temperature (T_R) for 1 h. The solutions of CS and PAN (Table 1) were mixed homogeneous using stirrer for 15 h. The mixing was followed by 30 min sonication to remove the bubbles. The mix solution was then poured into a petri dish and placed into oven for drying at 40 °C for 4 days. Afterward, the films were dried in the vacuum oven at 60 °C and -0.1 MPa until complete dryness. Dried films of CS/PAN were detached from the petri dish and stored into a closed plastic bag for characterization. The mixing and solution casting of CS and PAN is shown in Figure 1.

Preparation of sIPN Hydrogel Film

The crosslinking reaction of CS/PAN hydrogel Gel1 (C80/P20) was carried out by placing the hydrogel film on a

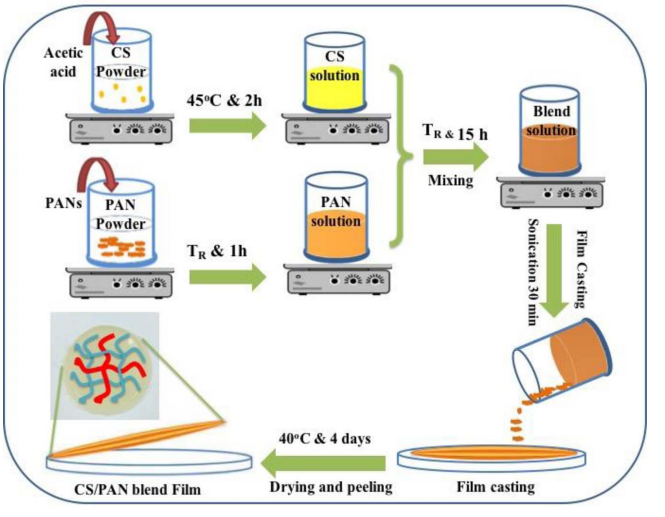

Figure 1. Schematic for preparation of CS/PAN hydrogel film.

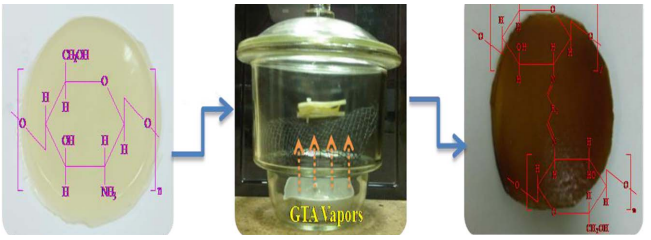

Figure 2. Preparation of the sIPN hydrogel and exposure of hydrogel to GTA vapors.

Table 1. Sample names and codes for CS/hydrogel films

CS/PAN hydrogel films		
Sample codes	CS wt%	PAN wt%
Gel1	80	20
sIPN hydrogel films		
Sample codes	Sample	Under 25 % GTA environment
Gel2	G-C80/P20	24 h
Gel3	G-C80/P20	48 h
Gel4	G-C80/P20	96 h

porous ceramic shelf. An aqueous solution of GTA (25 %) was added in a dish and the dish was placed at the bottom of the sealed desiccators at room temperature for different time duration of 24, 48, and 96 h. A schematic for the preparation of semi IPN hydrogel has been shown in Figure 2. After the reaction, the hydrogel samples were dried in a vacuum oven at 60 °C and -0.1 MPa for 24 h and stored for characterization. The samples names and codes are described in the Table 1.

FT-IR Study

FTIR spectra of the CS powder, PAN powder, CS/PAN blended and sIPN hydrogel films were taken by using FT-IR spectrometer (Bruker Vertex 70). For the FT-IR characterization, the KBr discs of the samples were prepared by mixing and grounding the samples with KBr powder in a mortar with a pestle. The mixture was then shaped into discs under hydraulic press. The samples discs were placed into FT-IR and spectral measurements were recorded in the wavenumber range of 400-4000 cm^{-1}. The data was processed by using Software OPUS 6.0 (Bruker), which was baselined by rubber band method (CO_2 and H_2O bands excluded).

Thermo Gravimetric Analysis

Thermal behavior of the blend and sIPN hydrogel films were studied by TGA (Q50, TA Instruments, US). The sample was placed in the platinum plate, weighed and heated at 10 °C/min in the temperature range (T_r) of 25 to 600 °C under N2 environment. The onset temperature (T_o), maximum degradation temperature (T_{max}) and half decomposition temperature ($T_{1/2}$) were obtained from the thermograms *via* a built in software in Q50 TA instrument.

Degree of Swelling

The degree of swelling of the CS/PAN blend and sIPN hydrogel films was calculated by equation (1). The samples were thoroughly dried under vacuum at 60 °C and -0.1 MPa to a constant weight. Each sample was then weighed and the weight is noted on the data sheet as dry weight. Each dried sample was separately immersed in a vial (at room temperature), which contained 15 mL of distilled water. The samples were taken out of the vials at regular intervals (5 mins to 2880 min), wiped between two filter papers (to remove the excess surface water) and then weighed. This weight is noted as swollen weight on the data sheet.

$$Swelling\ (\%) = \left(\frac{W_S - W_D}{W_D}\right) \times 100 \quad (1)$$

where W_S and W_D are the weights of the swollen and dried samples, respectively.

Stability Study

For the measurement of the degree of stability, the CS/PAN and sIPN hydrogel films were thoroughly dried under vacuum at 60 °C and -0.1 MPa to a constant weight. The dried samples were initially weighed and the observation is noted on the data sheet. After weighing, the samples were dipped into distilled water inside vials, separately and allowed to remain in the distilled water for different time intervals (i.e., 8, 24, 48, 72, and 96 h) at room temperature. The sample was taken out from each vial at a desired time interval, dried, weighed and the observation is noted on the data sheet. The degree of stability was calculated by using equation (2).

$$Stability\ (\%) = \left(\frac{W_2}{W_1}\right) \times 100 \quad (2)$$

where W_1 and W_2 are the initial and final weights of the dried hydrogel.

State of Water Study

The states of water in the CS/PAN blend and sIPN hydrogel films were measured using freeze drying technique. CHRIST freeze dryer (model ALPHA1-2 LD Plus) was used in these experiments. The initially dried and weighed samples were immersed in vials containing distilled water and allowed to swell until equilibrium. The equilibrium time was obtained from the swelling kinetics plots. The weight of each swelled sample was measured. The samples were place in the shelves of the freeze dryer for freezing at -40 °C for 20 min. This was followed by drying the samples at -40 °C and 1.6 Mbar for 60 min. To remove even the small traces of unbounded water from the films, the samples were further dried at -55 °C and 0.04 Mbar for 20 min. Finally, the samples were removed from the shelves and their weights

were measured.

The total amount of water (W_T) was calculated by subtracting the weight of dry sample (W_I) from the swollen sample (W_S). The percentages of total (W_T %), unbound (W_{UB} %) and bound water (W_B %) were determined using equations (3)-(5) [27]

$$W_T\,(\%) = \left(\frac{W_S - W_I}{W_S}\right) \times 100 \quad (3)$$

where W_T, W_S and W_I are the amounts of the total, swollen and initial dry weights of the sample, respectively

$$W_B\,(\%) = \left(\frac{W_F - W_I}{W_S}\right) \times 100 \quad (4)$$

where, W_F is the weight of freeze dried sample.

The amount of unbound water was determined by subtracting the amount of bound water from total water.

$$W_{UB}\,(\%) = W_T\,(\%) - W_B\,(\%) \quad (5)$$

where W_{UB}, W_T and W_B are the amounts of unbound, total and bound water, respectively.

Morphology Study

The morphologies of the freeze dried blend and sPIN hydrogel films were studied by using FE-SEM (FEI Quanta 200 (SEM-2)). To study the surface and cross section morphologies of the films, the films were fixed on to a sample holder with the aid of 12 mm diameter carbon tapes and coated with platinum in sputtering machine. After platinum coating the samples were examined under high vacuum.

Results and Discussion

Fourier Transform Infrared Spectroscopy (FTIR)

Figure 3 shows the FTIR spectra of the CS, PAN, blend (Gel1) and sIPN (Gel4) hydrogel films. The spectrum of CS shows the characteristics bands of -NH_2 stretching and hydroxyl group in the range of 3500-3450 cm^{-1}, amide I and amide III in the range of 1637-1650 cm^{-1} and at 1311 cm^{-1}, respectively (Figure 3(a)). The band at 1650 cm^{-1} was attributed to amide I for the remaining acetamide group in CS [28]. Figure 3(b) illustrates the typical FT-IR spectrum of the PAN [29]. The spectrum of PAN shows a sharp band at 2240 cm^{-1} for nitrile group (C≡N) [28]. The bands in the regions of 2870-2944, 1450-1460, 1350-1380, and 1220-1270 cm^{-1} are assigned to the aliphatic CH group vibrations of different modes in CH, CH_2, and CH_3, respectively [29]. Figure 3(c) shows the FTIR spectrum of the CS/PAN blend. No changes in the characteristic bands of CS and PAN were observed, which suggested a weak chemical interaction between the two polymers. Figure 3(d) shows the FTIR spectrum for sIPN (Gel4), in here a new doublet band at 1563 cm^{-1} and 1630 cm^{-1} was observed due to the formation of imine bonds (C=N). The appearance of this band is attributed to the reaction of amino groups in CS and aldehyde groups in GTA [28].

TGA Analysis

Figure 4((a) and (b)), and Table 2 indicates the thermal behavior of CS/PAN blend (Gel 1) and sIPN hydrogels films (Gel2, Gel3 and Gel4 (Table 1)). Thermal degradation of the blend and sIPN hydrogels film followed similar patterns. The weight loss (W_L) took place in two stages (Figure 4(a)). The first stage degradation for blend (Gel1) started at approximately 76 °C (onset temperature) and continued till 204 °C. The maximum degradation occurred at 109 °C with a W_L of around 65 %. The first stage degradation for the Gel2, Gel3 and Gel4 sIPN started at 98, 106, 113 °C (Figure 4(b) and Table 2), shifting their maximum degradation temperatures (T_{max}) to a higher side i.e. 138 °C, 152 °C, and 164 °C, respectively (Figure 4(b) and Table 2). The first stage W_L for Gel2, Gel3 and Gel4 sIPN at these temperatures were 81.4, 90, and 92 %, respectively. The increased W_L at this stage for the sIPN hydrogels films could be attributed to the increase in the amount of unreactive GTA [30], which is further attributed to the fact that GTA vapors could not sufficiently penetrated the surface of the film during crosslinking. The moisture loss for all the samples occurred below 100 °C [31]. The second stage degradation for Gel1, Gel2, Gel3 and Gel4 started at 271, 268, 276 and 299 °C, respectively. The W_L at this stage was 13 % for Gel1, 9.2 % for Gel2, 2.3 % for Gel3 and 8.5 for Gel4. The DTA curves (Figure 4(b)) showed slight low T_{max} for Gel2 as compared to Gel3 and Gel4 in the second stage. The half degradation or weight loss temperature ($T_{1/2}$) increased from 132 for Gel1 to 150 °C for Gel4 and the total residue weight % (W_R) decreased from 15 for Gel1 to 4.1 % for Gel4 (Table 2). From the above result, it is evident that thermal properties of the hydrogels films improved with increase in the films exposure time to crosslinker.

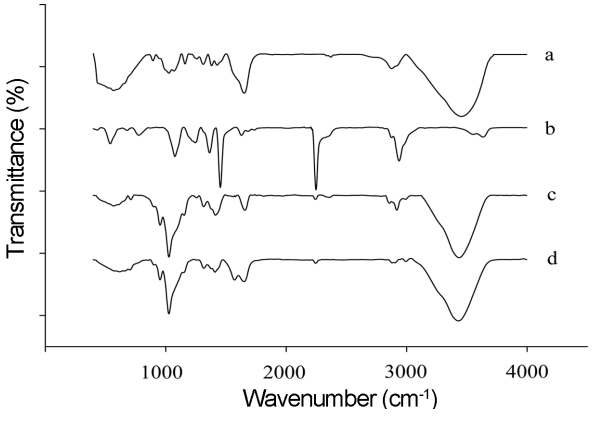

Figure 3. FTIR spectra of chitosan (a), PAN (b), Gel1 (c) and Gel4 (d).

Swelling Kinetics

Figure 5 illustrates the swelling kinetics of the blend (Gel1) and sIPN (Gel2-Gel4) hydrogel films as a function of exposure time. The inset plot shows the degree of swelling of the hydrogel films at equilibrium, whereas the digital images show the maximum and minimum swelled films of Gel1 and Gel 4. The degree of swelling for all the samples increased sharply until ~300 min and reached equilibrium at ~480 min. After the initial sharp swelling, the degree of swelling gradually decreased as the exposure time is increased and reached equilibrium. The initial sharp increase is attributed to the easily available hydrophilic sites on the films. Furthermore, Gel1 showed maximum degree of swelling (~2200 %) while Gel4 has the lowest degree of swelling (~1000). The increased degree of swelling in case of Gel1is attributed to the fact that the polymer chains could freely move and thus are offering a larger surface area and better matrix solvent interaction, hence allowing faster solvent diffusion and efficient and rapid swelling [32]. Whereas the decreased degree of swelling in case of Gel4 is attributed to increase in the extent of crosslinking, which restricted the movement of the polymer chains and formed a more compact structure. Our arguments are also supported by the results of the FE-SEM morphology study, which are discussed in the later section. This phenomena is more easily understandable from the steady decrease in the swelling (e.g., the degree of swelling of Gel2, Gel3 and Gel4 decreased as ~1460, ~1100, and ~1000, respectively) with increase in crosslinking.

The kinetics of swelling can be described by the following second order rate equations [33],

$$\frac{dW}{dt} = K(W_\infty - W)^2 \tag{7}$$

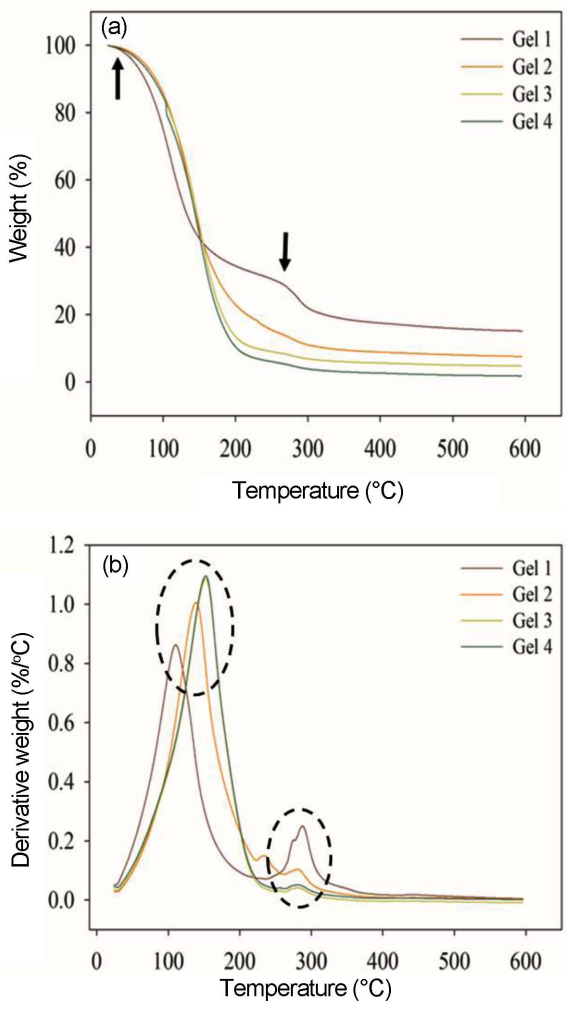

Figure 4. TGA thermogram (a) and DTA (b) curves of the hydrogels.

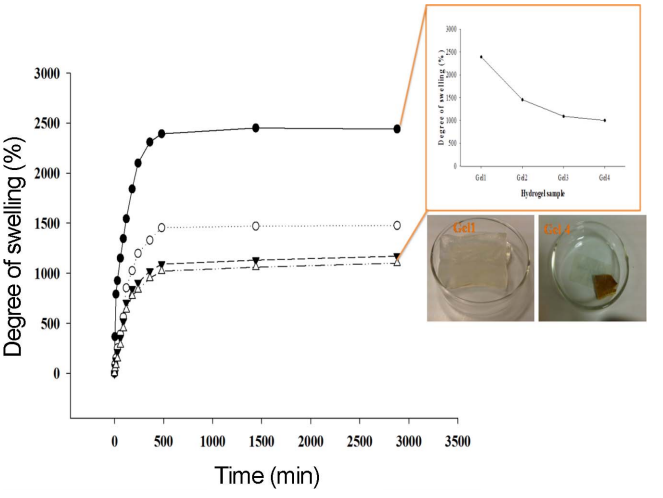

Figure 5. Swelling ratio of the hydrogels as function of time Gel1 (●), Gel2 (○), Gel3 (▼) and Gel4 (Δ).

Table 2. Degradation temperature for the semi-IPN hydrogel films

Samples	First stage				Second stage				$T_{1/2}$	W_R(%)
	T_r	W_L	T_{max}	T_o	T_r	W_L(%)	T_{max}	T_o		
Gel1	25-204	65	109	76	204-317	13	286	271	132	15
Gel2	25-226	81	138	98	226-350	9.2	281	268	145	7.5
Gel3	25-250	90	152	106	250-310	2.3	282	276	148	4.7
Gel4	25-253	92	164	113	200-320	8.5	304	299	150	4.1

$$\frac{t}{w} = \frac{1}{KW_\infty^2} + \frac{1}{W_\infty}t \quad (8)$$

$$\frac{t}{W} = A + Bt \quad (9)$$

where K, W_∞, W are the rate constants, the maximum (equilibrium) solvent uptake and the amount of the solvent absorbed at time t, respectively. $(W_\infty - W)$ is the swelling capacity. A $(=1/KW_\infty^2)$ and B $(=1/W_\infty)$ are the intercept and slope, respectively, of the t/W vs. t plot.

Equation (9) follows from the integration and rearrangement of equation (8). According to equation (9), the swelling data must fit a straight line with a slope of 1 $/W_\infty$ and an ordinate of $1/KW_\infty^2$.

Figure 6 depicts the linear regression ressults of the t/W vs. t plot. The resulting constants A and B are given in Table 3. The straight lines indicate that the swelling of hydrogels indeed followed second-order kinetics, where the rate of swelling at any time is directly proportional to the square of the swelling capacity. Note that similar to the equilibrium swelling, both K_∞ (rate of swelling) and W_∞ have maxima for Gel1 as shown in Table 3.

Stability Kinetics

Figure 7 shows the degree of stability (calculated with equation (2)) of the blend (Gel1) and sIPN (Gel2, Gel3 and Gel4) hydrogel films in an aqueous solution at neutral pH and upto 96 h. The sharp and continuous decrease in the degree of stability for the blend hydrogel film Gel1 could be attributed to the low physical interactions of CS and PAN polymers, hydrophilic nature and high susceptibility of the CS to degradation. The sIPN hydrogel film Gel4 showed better stability. The order of the degree of stability of the sIPN hydrogel films was observed as Gel2 < Gel3 < Gel4. The better stability of sIPN hydrogel films was attributed to the increased crosslinking of the CS due to the exposure of the films to crosslinker for a longer time. The slightly unusual behavior shown by sIPN hydrogel film Gel2 could be attributed to some handling issue during experiment, which could be easily improved.

Table 3. Linear regression kinetic parameters results of Figure 6

Sample	A/min W-1a	B/ W-1	K/ (W min^{-1})	W_∞/W
Gel1	0.0194	0.0004	7.1797	2440
Gel2	0.0688	0.0006	3.8125	1476
Gel3	0.0832	0.0008	3.4669	1170
Gel4	0.1121	0.0009	2.9867	1100

[a] W is the percentage of the amount of the solvent absorbed.

States of Water in the Hydrogels

Table 4 shows the states of water for the blend (Gel1) and sIPN (Gel2-Gel4) hydrogel films. There are three types of waters in hydrogels i.e. unbound (freezing), intermediate (freezing-bound) and bound (nonfreezing) [27,33]. Unbound (freezing (W_{UB})) water does not form hydrogen bonds with the polymer molecules and shows greater degree of mobility, while bound (nonfreezing (W_{NF})) water forms hydrogen bonds and shows little or no mobility [34,35]. Intermediate (freezing-bound (W_{FB})) water interacts with the polymer molecules but show mobility. Thus, W_{UB} is represented by $W_{UB}+W_{FB}$. The amounts of the different states of water, listed in Table 4, were calculated using equation (4)-(6). Similar to the degree of swelling, unbound water has a maximum for Gel1 (52.3 %). In contrast, the W_B did not change much which is attributed to the nearly constant contact area that is maintained between water and the hydrogel films. For sIPN hydrogel films, similar to the equilibrium, the unbound water has a maximum for Gel2 followed by Gel3 and Gel4. W_B increased gradually with respect to GTA exposure time. The increase in W_B showed that the contact area between water and sIPN hydrogel films is increased due to the induction of new water contacting points in these

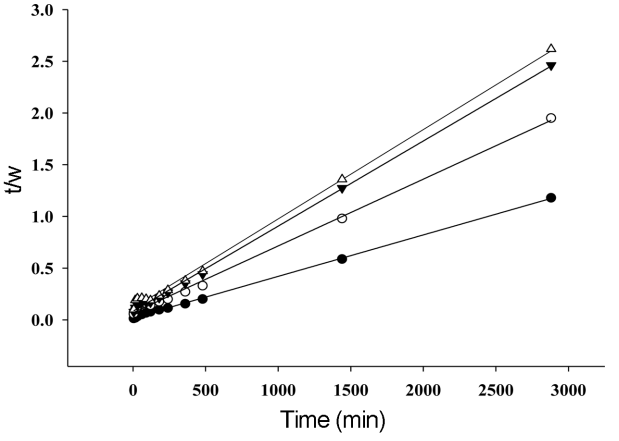

Figure 6. (a) Linear regression (using equation (8)) of the swelling curves for (●) Gel1, (○) Gel2, (▼) Gel3, and (Δ) Gel4.

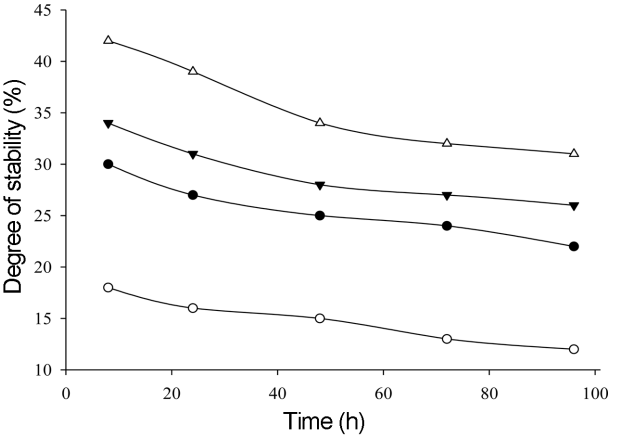

Figure 7. Degree of stability of the hydrogels at different intervals Gel1 (●), Gel2 (○), Gel3 (▼), and Gel4 (Δ).

Table 4. The amount and states of water in the hydrogel films using equation (3)-(5)

Sample	W_T (%)	W_B (%)	W_{UB} (%)
Gel1	94.2	41.9	52.3
Gel2	74.0	48.0	26.0
Gel3	73.5	49.5	24.0
Gel4	73.0	52.0	21.0

hydrogel films. The crosslinked and compact structure of Gel3 and Gel4 resulted in low W_T and W_{UB}. According to literature data [34,35] the amount of W_B in different polymer-water systems varies both with chemical as well as higher-order structure of a polymer. Thus, it can be inferred that the difference in values of W_T, W_B and W_{UB} for Gel and sIPN hydrogels resulted both from the changes in hydrophilicity or hydrophobicity as well as crystallinity of non-crosslinked and crosslinked structures of the hydrogel films.

Morphology of the Hydrogel Films

Figure 8 shows the FE-SEM micrographs (surface and cross section) and digital images of the freeze dried hydrogel films (e.g., Gel1 and Gel4). The surfaces morphologies of both the hydrogel films are homogeneous and smooth with little porosity and small blisters (Figure 8(a), (b)). The homogeneous (no phase separation) and smooth surface is attributed to the good miscibility between CS and PAN. The cross-section surface showed open morphology with sufficient porosity for Gel1 (Figure 8(a')), which is attributed to the mobility of the CS polymer chains, high degree of swelling and the presence of sufficient amount of unbound water. The open structure of hydrogel films might be helpful for the sorption of toxic materials such as dyes from the wastewater. The cross section surface for Gel4 showed a more compact structure and very little porosity. As discussed earlier, compact structure formation is attributed to increased crosslinking of the CS, which limited the polymer chains mobility.

Conclusion

sIPN hydrogels composed of CS and PAN have been prepared with different exposure time (0 h, 24 h, 48 h and

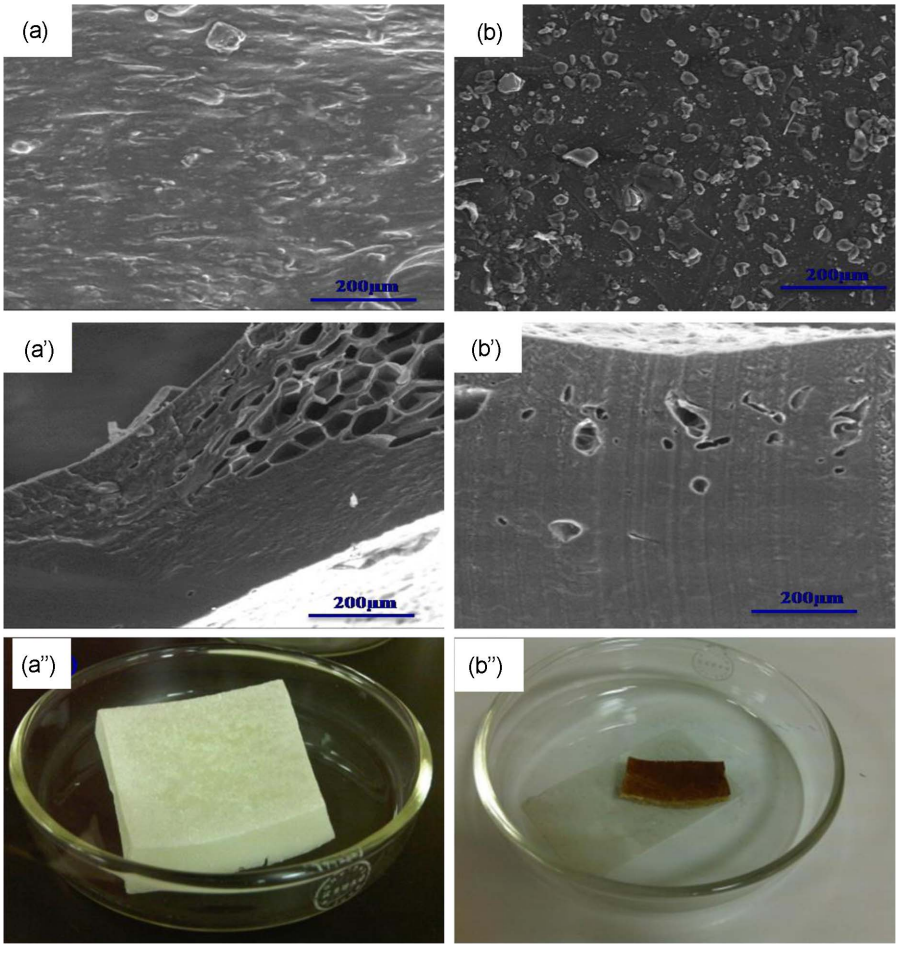

Figure 8. FE-SEM micrographs and digital images of hydrogels: Gel1 surface morphology (a), cross-section surface (a') and digital image (a"), and Gel 4 surface morphology (b), cross-section surface (b') and digital image (b").

96 h) to GTA vapors. The effect of crosslinking on the degree of swelling, swelling kinetics, aqueous and thermal stabilities, state of water and morphology of sPIN has been studied. The results revealed that crosslinking affected the degree of swelling and showed no affect on the swelling kinetics of the hydrogel films; which followed second order kinetics eqn. Aqueous and thermal and stabilities were improved with increase in crosslinking time. A change in the W_B and W_{UB} water was observed for the hydrogel samples (Gel1-Gel4). This was attributed to the changes in the contact area between water and hydrogel films.

Acknowledgment

The authors would like to extend their sincere appreciation to the Deanship of Scientific Research (DSR) at King Saud University for its funding of this research through the Research Group no RG-1437-029.

References

1. R. Pó, *J. Macromol. Sci., Part C*, **34**, 607 (1994).
2. H. Warson, *Polym. Int*., **49**, 1548 (2000).
3. N. A. Peppas and A. R. Khare, *Adv. Drug Deliv. Rev*., **11**, 1 (1993).
4. D. Kim and K. Park, *Polymer*, **45**, 189 (2004).
5. J. Yang, J. Chen, D. Pan, Y. Wan, and Z. Wang, *Carbohydr. Polym*., **92**, 719 (2013).
6. S. Chaterji, I. K. Kwon, and K. Park, *Prog. Polym. Sci*., **32**, 1083 (2007).
7. E. S. Dragan, A. I. Cocarta, and M. Gierszewska, *Colloid Surf. B-Biointerfaces*, **139**, 33 (2016).
8. N. Bhattarai, J. Gunn, and M. Zhang, *Adv. Drug. Deliv. Rev*., **62**, 83 (2010).
9. H. Saito, A. Sakurai, M. Sakakibara, and H. Saga, *J. Appl. Polym. Sci.*, **90**, 3020 (2003).
10. D. S. Franklin and S. Guhanathan, *Iran. Polym. J*., **23**, 809 (2014).
11. S. J. Kim, S. G. Yoon, K. B. Lee, Y. D. Park, and S. I. Kim, *Solid State Ion.*, **164**, 199 (2003).
12. M. Mucha, *React. Funct. Polym.,* **38**, 19 (1998).
13. A. Sionkowska, M. Wisniewski, J. Skopinska, C. J. Kennedy, and T. J. Wess, *Biomaterials*, **25**, 795 (2004).
14. M. Jafarkhani, A. Fazlali, F. Moztarzadeh, and M. Mozafari, *Iran. Polym. J.*, **21**, 713 (2012).
15. D. K. Singh and A. R. Ray, *J. Appl. Polym. Sci.*, **66**, 869 (1997).
16. S. Yoshikawa, T. Takayama, and N. Tsubokawa, *J. Appl. Polym. Sci.*, **68**, 1883 (1998).
17. V. M. Correlo, L. F. Boesel, M. Bhattacharya, J. F. Mano, N. M. Neves, and R. L. Reis, *Mater. Sci. Eng., A*, **403**, 57 (2005).
18. D. K. Kweon and D. W. Kang, *J. Appl. Polym. Sci.*, **74**, 458 (1999).
19. M. Zhang, X. H. Li, Y. D. Gong, N. M. Zhao, and X. F. Zhang, *Biomaterials*, **23**, 2641 (2002).
20. E. Jain and A. Kumar, *J. Biomater. Sci. Polym. Ed*., **20**, 877 (2009).
21. S. C. Angadi, L. S. Manjeshwar, and T. M. Aminabhavi, *Int. J. Biol. Macromol*., **47**, 171 (2010).
22. E. S. Dragan, *Chem. Eng. J*., **243**, 572 (2014).
23. E. A. El-Hefian, M. M. Nasef, and A. H. Yahaya, *J. Chem. Soc. Pak*, **36**, 11 (2014).
24. F. S. Al-Mubaddel, S. Haider, M. O. Aijaz, A. Haider, T. Kamal, W. A. Almasry, M. Javid, and S. U.-D. Khan, *Polym. Bull.*, 1 (2016).
25. J. D. Schiffman and C. L. Schauer, *Biomacromolecules*, **8**, 594 (2007).
26. J. L. Vondran, W. Sun, and C. L. Schauer, *J. Appl. Polym. Sci*., **109**, 968 (2008).
27. V. R. Patel and M. M. Amiji, *Pharm. Res*., **13**, 588 (1996).
28. S. J. Kim, S. R. Shin, Y. M. Lee, and S. I. Kim, *J. Appl. Polym. Sci.*, **87**, 2011 (2003).
29. A. V. Korobeinyk, R. L. D. Whitby, and S. V. Mikhalovsky, *Eur. Polym. J.*, **48**, 97 (2012).
30. M. Khalid, F. Agnely, N. Yagoubi, J. Grossiord, and G. Couarraze, *Eur. J. Pharm. Sci*., **15**, 425 (2002).
31. R. Tripathi and B. Mishra, *AAPS Pharm. Sci. Technol.*, **13**, 1091 (2012).
32. P. M. D. L. Torre, Y. Enobakhare, G. Torrado, and S. Torrado, *Biomaterials*, **24**, 1499 (2003).
33. S. Haider, S.-Y. Park, and S.-H. Lee, *Soft Matter*, **4**, 485 (2008).
34. X. Qu, A. Wirsén, and A. C. Albertsson, *Polymer*, **41**, 4589 (2000).
35. H. Hatakeyama and T. Hatakeyama, *Thermochim. Acta*, **308**, 3 (1998).